



SOIL NON-LINEAR BEHAVIOR AND HYSTERETIC DAMPING IN THE SPRING-DASHPOT ANALOG

Nikolaos OROLOGOPOULOS¹ and Dimitrios LOUKIDIS²

ABSTRACT

This paper presents results from numerical simulations of footing vibration examining the effect of the variation of soil shear stiffness and hysteretic damping ratio with shear strain amplitude on the values of the spring and dashpot coefficients of the Lysmer's analog. Following validation of the numerical methodology against existing semi-analytical solutions found in the literature, a series of parametric finite element analyses are performed for vertical oscillation, horizontal oscillation and rocking of strip footings and vertical oscillation of circular footings, resting on a the free surface of a homogeneous half-space. In validation process, the soil is assumed to be a linearly elastic material, while, in the subsequent parametric study, the soil is modeled as a non-linear material following a simple hyperbolic stress-strain law with hysteresis. The study aims at establishing relationships for the determination of the spring stiffness and the dashpot coefficients for footings on fine grained soils as a function of the normalized foundation motion amplitude.

INTRODUCTION

The role of the foundation soil in seismic response analysis of structures is traditionally represented by simple spring and dashpot models. In most cases of soil-structure interaction simulations, the foundation soil is assumed to have constant shear stiffness (shear modulus G) and constant hysteretic damping ratio ξ_h . Numerous research studies have produced formulas and charts for the determination of the spring coefficient K and dashpot coefficient C for all possible modes of oscillation of shallow foundations, as functions of the footing size and geometry, soil elastic parameters, shear wave velocity V_s and oscillation angular frequency ω (e.g., Lysmer 1965; Karashudhi et al. 1968; Luco and Westmann 1971; Veletsos and Wei 1971; Veletsos and Verbič 1973; Gazetas and Roesset 1976, 1979; Gazetas 1983; Dobry and Gazetas 1986). The spring coefficient is usually expressed as the product of the static stiffness K_{stat} and a dynamic stiffness factor k that is a function of ω . The dashpot in such models represents mainly the radiation damping (i.e., the energy loss due to the emission of mechanical waves to the elastic half-space). The energy consumed at a material point, namely the hysteretic damping, is taken into account by applying the principle of correspondence as follows (Dobry and Gazetas 1986):

$$K(\xi_h) = K - \omega C \xi_h \quad (1)$$

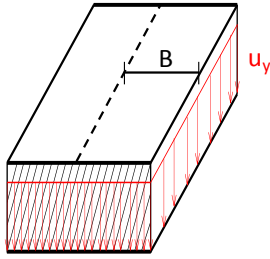
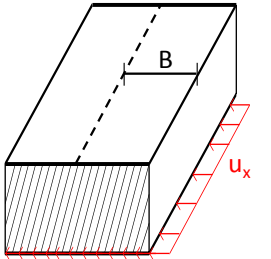
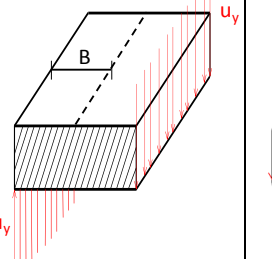
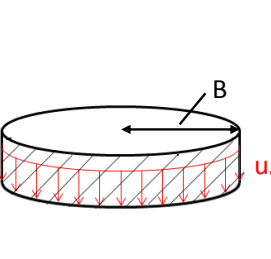
$$C(\xi_h) = C + \frac{2K\xi_h}{\omega} \quad (2)$$

¹ Research Assistant, University of Cyprus, Nicosia, Cyprus, norologopoulos@gmail.com

² Assistant Professor, University of Cyprus, Nicosia, Cyprus, loukidis@ucy.ac.cy

It is well known that the actual soil behavior is strongly non-linear, resulting in gradual reduction of secant shear modulus and increase of hysteretic damping ratio as the amplitude of shear strain γ increases (Vucetic and Dobry 1991). Hence, it is expected that K would decrease and C would increase with increasing amplitude of foundation displacement (or rotation for the rocking mode). This fact is currently neglected in the standard spring-dashpot models that represent the foundation soil in soil-structure interaction analyses in engineering practice. Nonetheless, several research efforts have focused on introducing soil non-linearity in soil-structure interaction analysis through macro-element modeling (e.g., Paolucci 1997; Cremer et al. 2001; Houlsby et al. 2005; Chatzigogos et al. 2009). Moreover, significant attention has been drawn recently to the potential benefits to the structural seismic response coming from the development of inelastic soil deformation under the foundations and from the corresponding energy dissipation (e.g., Mergos and Kawashima 2005; Anastasopoulos et al. 2010; Kourkoulis et al. 2012; Zafeirakos and Gerolymos 2013).

Table 1. Foundation geometries and vibration modes considered in the finite element analyses.

			
strip footing – vertical oscillation (plane strain)	strip footing – horizontal oscillation (plane strain)	strip footing - rocking (plane strain)	circular footing - vertical oscillation (axisymmetric)

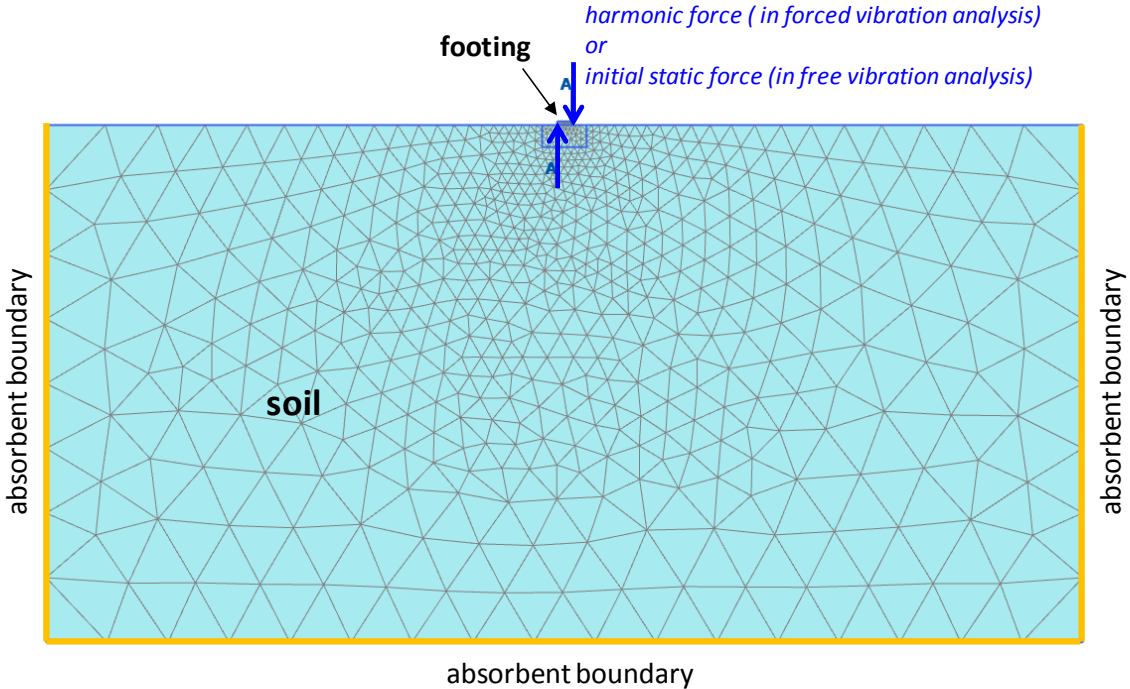


Figure 1. Typical finite element mesh and boundary conditions used in analyses of strip footing excited in rocking.

This paper investigates the effect of the variation of soil stiffness and hysteretic damping ratio, as a function of the motion amplitude, on the values of the spring and dashpot coefficients for shallow foundation resting on the free surface of a homogeneous half-space. For this purpose, series of parametric analyses were performed using the finite element code PLAXIS 2D (Brinkgreve et al. 2011) for vertical, horizontal and rocking oscillations of strip footings and vertical oscillation of circular footings (Table 1), in which the soil mechanical behavior is represented by a hyperbolic stress-strain law that predicts hysteresis. The asymptotic strength of the hyperbolic law is assumed to be independent of the mean effective stress. Hence, the analysis results are applicable to fine grained soils (e.g., clays, silts) under undrained conditions. In order to ensure that the employed numerical methodology is capable of accurately simulating the problem at hand, an initial set of simulations was performed considering the ground as a linearly elastic medium with constant hysteretic damping ratio and the results were compared with existing semi-analytical solutions (e.g. Dobry and Gazetas 1986).

VALIDATION OF FINITE ELEMENT APPROACH

Simulations are first performed assuming that the soil is a linearly elastic medium in order to validate the finite element methodology. Finite element results are compared with the predictions of the spring-dashpot model for which K and C were calculated using the formulas and charts by Gazetas (1983) and Dobry & Gazetas (1986), which are based on semi-analytical solutions and, thus, can be considered rigorous. A large number of analyses were done for different values of Poisson's ratio, oscillation frequency and hysteretic damping ratio. The hysteretic damping of the soil was introduced in the analyses through Rayleigh damping:

$$C_{\text{Rayleigh}} = \alpha \mathbf{M} + \beta \mathbf{K} \quad (3)$$

where \mathbf{M} and \mathbf{K} are the global mass and stiffness matrices of the part of the finite element model occupied by the soil (no material damping is assigned to the footing). The parameters α and β are usually set to values equal to $\xi_{\text{target}}\omega$ and $\xi_{\text{target}}/\omega$, respectively, where ξ_{target} is the desired material damping ratio ξ_h at the predominant oscillation frequency ω of the system. These α and β values essentially divide the total contribution to the material damping into two equal parts, one pertaining to the mass (mass proportional Rayleigh damping) and the other pertaining to the stiffness (stiffness proportional Rayleigh damping). However, this approach is not suitable for problems involving wave propagation in a continuum, as it will be shown in the following paragraphs.

A typical finite element mesh is shown in Fig. 1, consisting of 15-noded triangular elements. Absorbent boundary conditions are assigned to the bottom and lateral boundaries in order to diminish reflection of the waves emitted by the foundation and achieve half-space consistent radiation damping as much as possible. The footing has a very high Young's modulus (practically rigid) and is fully attached to the ground, i.e. no interface elements are placed between soil and footing. Two sets of simulations were performed: a) forced vibration analysis and b) free vibration analysis. In forced vibration analysis, the footing is excited by a harmonic (sinusoidal) force time history of constant amplitude and frequency. The force is applied at the center of the footing in the case of vertical or horizontal excitation, while a pair of vertical forces of opposite direction are applied at the edges of the strip footing in the case of rocking in order to generate moment loading (Fig. 1). In horizontal oscillation analyses, the footing is prevented from moving vertically or rotating. Accordingly, in rocking analyses, the center of the footing is prevented from moving vertically or horizontally. These footing boundary conditions were applied in order to establish pure horizontal motion and pure rocking, which would otherwise be impossible due to the well known coupling between these two modes of oscillation.

In free vibration analysis, the footing is first loaded statically, and, subsequently, the loading is released (set to zero) instantaneously in order to allow the footing to vibrate freely. The mass of the footing was selected such that the resulting motion frequency is in the range of 3Hz to 12Hz. A typical response obtained from free vertical vibration analysis of a circular footing on soil with large hysteretic damping is shown in Fig. 2. It was observed that the free vibration analyses give a more

clear picture than forced vibration analyses with respect to the damping in the soil-foundation system and allow direct comparisons with semi-analytical solutions. The static part of these analyses was helpful also in making comparisons regarding the static stiffness of the system and in deciding the size of the analysis domain. This was particularly important for vertically or horizontally loaded strip footings because, in these cases, the footing displacement is sensitive to the distance of the boundaries from the footing.

The finite element results compare well with spring-dashpot analog predictions based on Gazetas (1983), Dobry and Gazetas (1986) and the principle of correspondence, with differences in the amplitude of forced vibrations not exceeding 5%. The errors are even smaller in analyses with $\zeta_h=0\%$, indicating that the finite element modeling in terms of absorbent boundaries and size of analysis domain can adequately simulate the correct radiation damping. However, the good agreement between the finite element method (FEM) and the spring-dashpot analog based on rigorous semi-analytical solutions is achieved on the condition that no mass proportional damping is used and the entire material damping comes from the stiffness proportional term by setting $\alpha=0$ and $\beta=2\zeta_h/\omega$ in Eq. (3). In fact, setting the Rayleigh damping to be both mass and stiffness proportional, as usually done in structural engineering practice, leads to a severe underestimation of the hysteretic damping of the soil, as shown in the example of Fig.2.

Rayleigh damping has been originally proposed and is suitable for single degree of freedom systems. The fact that the use of mass proportional damping in time domain analysis of multi-degree of freedom systems is problematic has been highlighted by Hall (2006). Mass proportional damping generates viscous forces (which consume energy) that are proportional to the absolute velocity of each individual node of the system, as if the material point moves inside a viscous fluid exerting drag forces. On the contrary, stiffness proportional damping generates damping forces that are proportional to the relative motion (relative velocity) of neighboring nodes and is, thus, related to shear straining. Hence, the stiffness proportional Rayleigh damping is closer to the physics of hysteretic damping in problems involving wave propagation in a continuum. In such problems, in-phase “single block” motion of the entire system is minimal and relative-differential motions dominate, and, as a result, the mass proportional component of the Rayleigh damping is undermobilized. As a consequence, if Eq. (3) is used with $\alpha=\zeta_h\omega$ and $\beta=\zeta_h/\omega$, the overall hysteretic damping will be underestimated, as shown in Fig. 2. The excellent agreement between FEM (with purely stiffness proportional Rayleigh damping) and the spring-dashpot analog is observed in all examined modes of vibration, independently of soil elastic properties, motion frequency and ζ_h value. So, it can be said that the principle of correspondence (Eq. 1 and 2) applies flawlessly to the investigated boundary value problems.

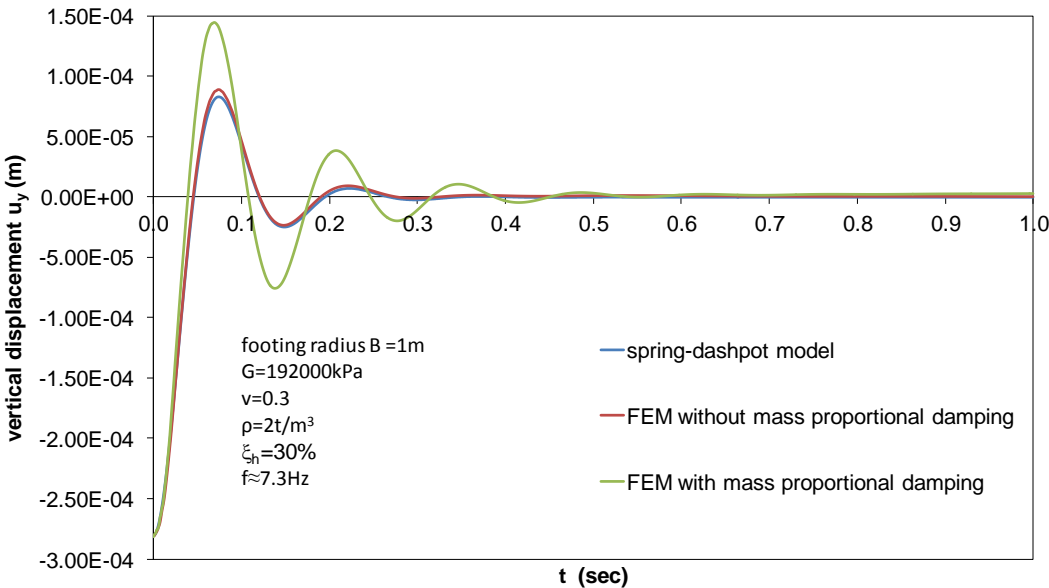


Figure 2. Comparison of the displacement time history of free vertically oscillating circular footing predicted by the spring-dashpot model and finite element analyses with and without mass proportional Rayleigh damping.

SOIL NON-LINEAR BEHAVIOR

The constitutive model used in the non-linear finite element analyses is the model available in PLAXIS 2D called *Hardening Soil model with small strain stiffness* (HSsmall). This model combines a shear yield surface (and a hardening cap) with pre-yield non-linear elastic behavior, thus being able to take into account the reduction of stiffness with shear strain and also predict hysteretic behavior. More specifically, before yielding, the material follows the hyperbolic law presented by Duncan and Chang (1970), as modified by dos Santos and Correia (2001). The modified expression of dos Santos and Correia (2001) for the secant shear modulus G has the following form:

$$\frac{G}{G_{\max}} = \frac{1}{1 + 0.385 \frac{\gamma}{\gamma_{0.7}}} \quad (4)$$

where $\gamma_{0.7}$ is the shear strain at which the secant shear modulus G is reduced to 72.2% of its initial (maximum) value G_{\max} . During unloading and reloading, the pre-yield formulation of HSsmall obeys the first and second Masing rules (Kramer 1996). In this study, our intention is to model soil behavior using purely the aforementioned hyperbolic law. In order to ensure that the plastic components of the constitutive model (yield surfaces, flow rule, e.t.c.) play no role on the material response, the material cohesion was set to a value twice the strength asymptote predicted by the hyperbolic law. Moreover, the soil friction angle is set equal to zero. As such, the FEM simulation results are meant to be valid for saturated fine grained soils (e.g., clays and silts). Fig.3 shows an example of the hysteresis loop predicted by the constitutive model in simple shear.

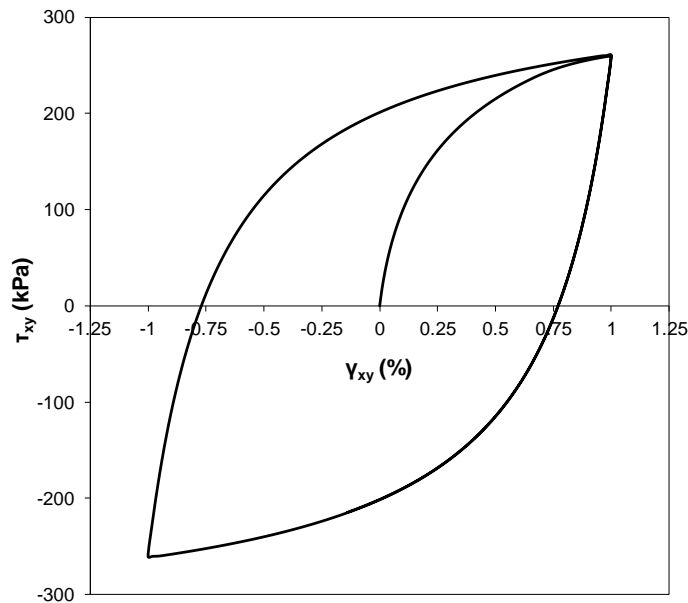


Figure 3. Hysteresis loop of soil material under simple shear loading as predicted by HSsmall.

The parameter $\gamma_{0.7}$ controls the curvature of the shear stress-strain response (backbone curve). This allows to fit, to the extent possible, the G/G_{\max} vs. γ and ξ_h vs. γ curves predicted by the HSsmall model to the experimental curves of Vucetic and Dobry (1991) for various values of the soil plasticity index PI. Three different PI values are considered in this study, PI=5, 20 and 40, with the corresponding $\gamma_{0.7}$ values that fit the Vucetic and Dobry (1991) curves being 0.00025, 0.0005 and 0.0008, respectively. The hyperbolic law of Eq. (4) yields zero hysteretic damping for very small shear strain amplitudes. On the other hand, experimental studies show that there is a minimum non-zero

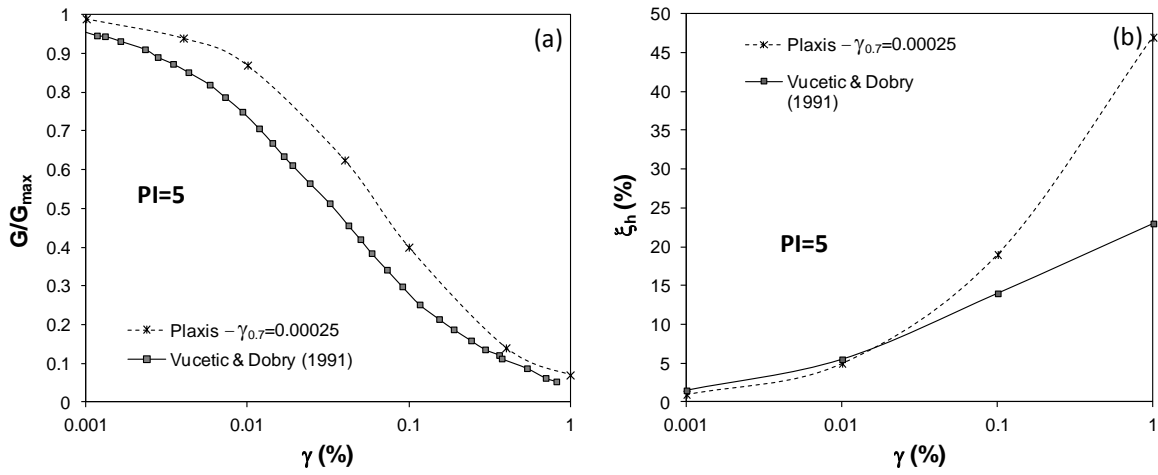


Figure 4. Comparison of experimental curves and HSsmall model predictions for PI=5.

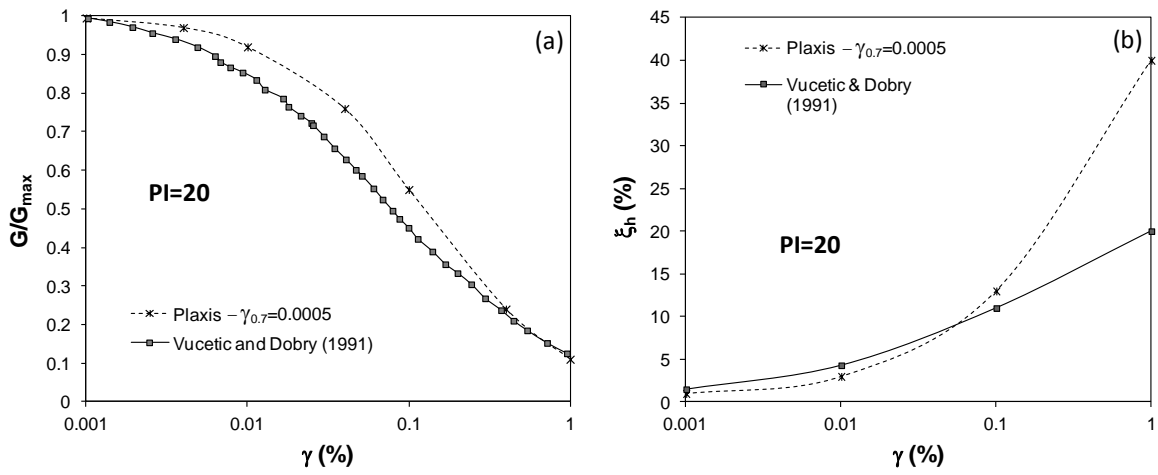


Figure 5. Comparison of experimental curves and HSsmall model predictions for PI=20.

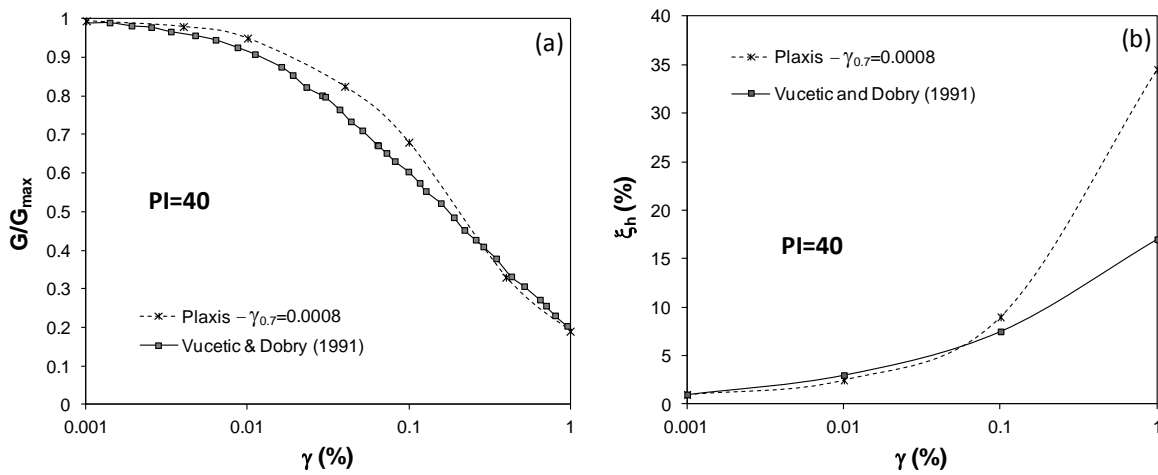


Figure 6. Comparison of experimental curves and HSsmall model predictions for PI=40.

value for ξ_h even at practically zero shear strain. Hence, along with HSsmall, a small amount of Rayleigh damping (stiffness proportional) was assigned to the soil in order to achieve a minimum ξ_h of 1%.

Figs. 4 through 6 compare HSsmall predictions in simple shear at material point level against the experimental observations (Vucetic and Dobry 1991). Effort was made to have the closest possible agreement in terms of both G/G_{max} vs. γ and ξ_h vs. γ curves. As a result, the G/G_{max} reduction is generally under-predicted at the small strain range in order to not excessively over-predict ξ_h . Yet, the over-prediction of ξ_h at $\gamma > 0.1\%$ is inevitably large. All non-linear analyses were performed for Poisson's ratio $\nu = 0.495$, assuming that the fine grained soil is fully saturated by capillary suction or by being under the water table.

NON-LINEAR ANALYSIS

The non-linear finite element analyses focus mainly on the effects of foundation size (half-width B ranging from 0.5m to 4m), G_{max} (50, 100 and 200MPa), PI (5, 20 and 40) and oscillation frequency f (in the range 3Hz to 12Hz). Given the values assumed for the parameter $\gamma_{0.7}$ of the hyperbolic law, the (asymptotic) undrained shear strength s_u of the soil ranges from 32kPa to 416kPa, and the corresponding G_{max}/s_u ratio from 480 to 1540. First, static parametric analyses were performed, in which the footing was loaded statically in order to obtain the reduction of the equivalent secant spring coefficient K_{equ} and establish curves of K_{equ}/K_{max} as a function of the normalized foundation displacement amplitude $u/2B$ (B : footing half-width). K_{max} is the spring coefficient corresponding to the maximum shear modulus G_{max} .

To determine the equivalent hysteretic damping ratio $\xi_{h, equ}$ of the soil-foundation system, free vibration analyses were performed for various levels of initial load amplitude. For each analysis, the total damping ratio ξ_{tot} of the system (radiation + hysteretic) was first extracted from the displacement time history (Fig. 7) using the well known logarithmic decrement method:

$$\xi_{tot, (n)} = \frac{\ln(u_n / u_{n+1})}{\sqrt{[\ln(u_n / u_{n+1})]^2 + 4\pi^2}} \quad (5)$$

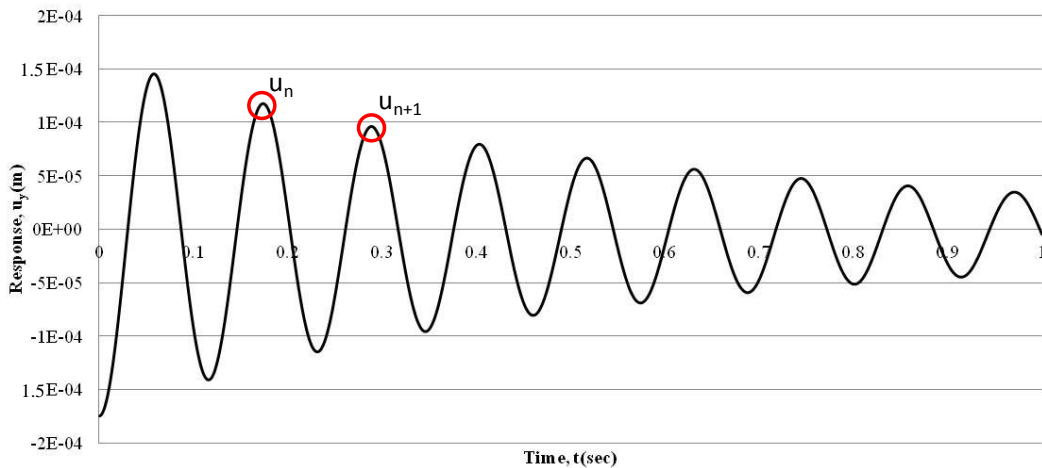


Figure 7. Determination of the damping ratio of a system from free vibration response.

The representative displacement amplitude corresponding to $\xi_{tot, (n)}$ (ξ_{tot} value calculated for the n^{th} cycle) is assumed to be equal to $u_{(n)} = (u_n + u_{n+1})/2$. Given Eq. (1), Eq. (2) and that $\xi_{tot} = 0.5C(\xi_h)\omega / K(\xi_h)$, the equivalent hysteretic damping ratio of the soil-foundation system can be determined from the following equation:

$$\xi_{h, \text{equ}} = \frac{K_{\text{equ}} k \xi_{\text{tot}}^2 - 0.5 \omega C}{K_{\text{equ}} k + \omega C \xi_{\text{tot}}} \quad (6)$$

with C and k obtained from Dobry and Gazetas (1986) and the K_{equ} value corresponding to $u_{(n)}$. It was observed that the $\xi_{h, \text{equ}}$ yielded by Eq. (6) was very close to the value obtained if we assume simple superposition of radiation and hysteretic damping:

$$\xi_{h, \text{equ}} \approx \xi_{\text{tot}} - \xi_{\text{rad}} = \xi_{\text{tot}} - \frac{C \omega}{2 K_{\text{equ}} k} \quad (7)$$

There are several pairs of displacement amplitude in a free vibration decay (such as the one shown in Fig. 7) that can be used for the calculation of $\xi_{h, \text{equ}}$. The earlier cycles yield larger damping ratios since they correspond to larger displacement amplitudes (and, consequently, larger average shear strain in the soil in the vicinity of the footing) than later cycles. By bringing together these results from several analyses in a graph, scatter plots are formed, as shown in Fig.8. It is interesting to note that the trend lines that fit closely the data points are actually linear functions of the footing displacement (or rotation θ in this particular case); they appear curved due to the logarithmic scale of the horizontal axis. Such trend lines of $\xi_{h, \text{equ}}$ vs. $u/2B$ are plotted in Fig. 9 and 10 for all parametric analyses performed for vertical oscillation of circular footing and rocking of strip footing, along with the respective stiffness reduction curves from static analyses.

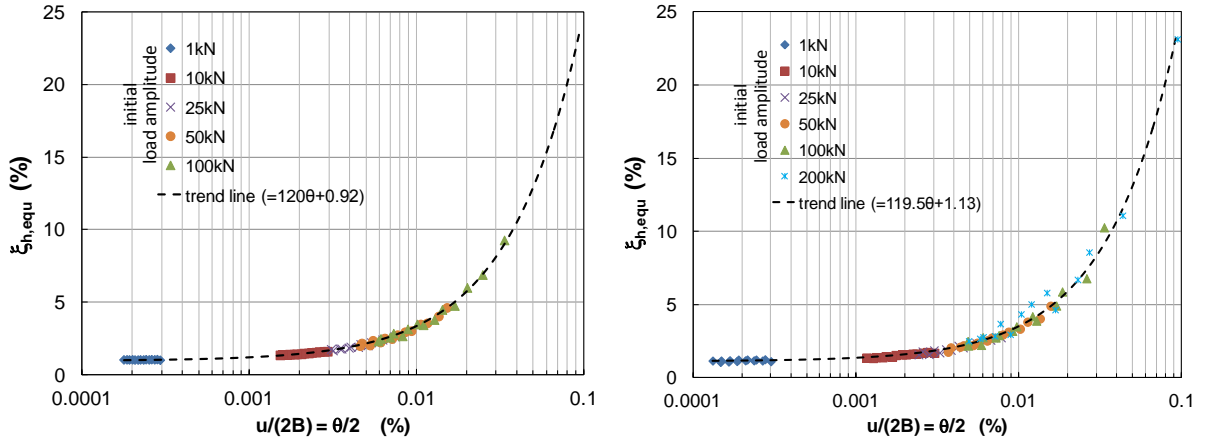


Figure 8. Scatter plots of equivalent hysteretic damping ratio $\xi_{h, \text{equ}}$ as a function of the normalized footing edge displacement amplitude $u/2B$ for strip footing in rocking from analyses with: a) $B=0.5\text{m}$, $G_{\text{max}}=200\text{MPa}$, $\text{PI}=20$, $f=12\text{Hz}$, b) $B=1\text{m}$, $G_{\text{max}}=100\text{MPa}$, $\text{PI}=20$, $f=6\text{Hz}$

Due the inherently very large radiation damping exhibited in the case of vertically or horizontally oscillating footings, extraction of $\xi_{h, \text{equ}}$ from free vibration analyses for these two modes was found unreliable. This is because of the very small displacement amplitudes left after the first cycle as a result of extreme decay. Moreover, the absorbent boundaries in the vertical or horizontal free vibration analyses exhibited significant permanent displacements. For these reasons, the $\xi_{h, \text{equ}}$ for these two strip footing oscillation modes was extracted from the area of the load-displacement hysteresis loop from analyses where the footing was cycled quasi-statically, as shown in Fig. 11. The resulting equivalent spring stiffness and hysteretic damping ratio as functions of $u/2B$ are presented in Figs. 12 and 13. The constitutive model employed herein predicts zero hysteretic damping at very small shear strains and, thus, quasi-static analyses produce zero $\xi_{h, \text{equ}}$ for very small footing motion amplitudes. Hence, a value of 1% was added to the quasi-static FEM results in order to be able to make direct comparisons between Figs. 12 and 13 and Fig. 9 and 10.

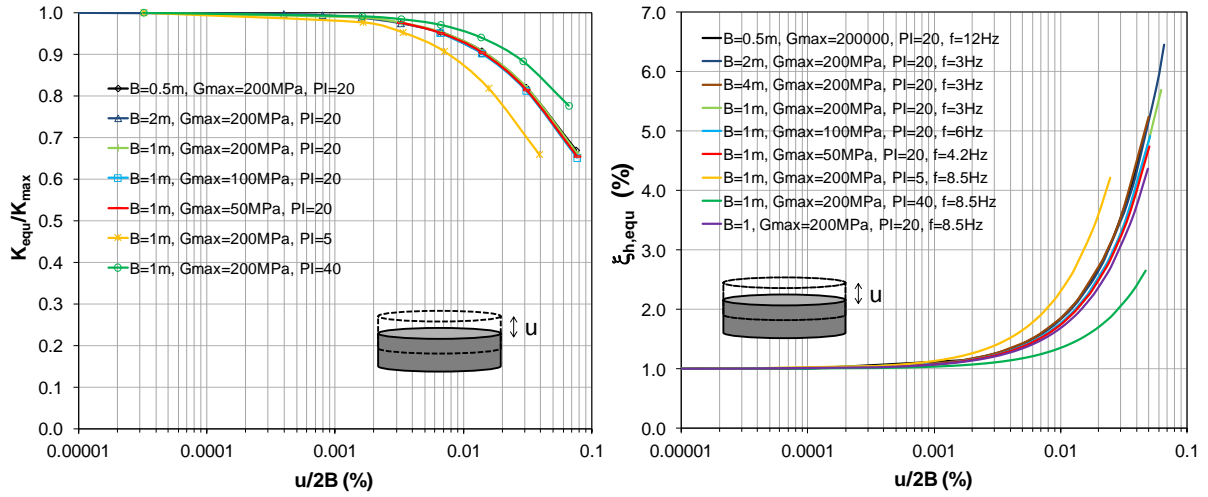


Figure 9. Equivalent spring stiffness K_{equ} and hysteretic damping ratio $\xi_{h, equ}$ as functions of the normalized footing displacement amplitude $u/2B$ for circular footing in vertical oscillation.

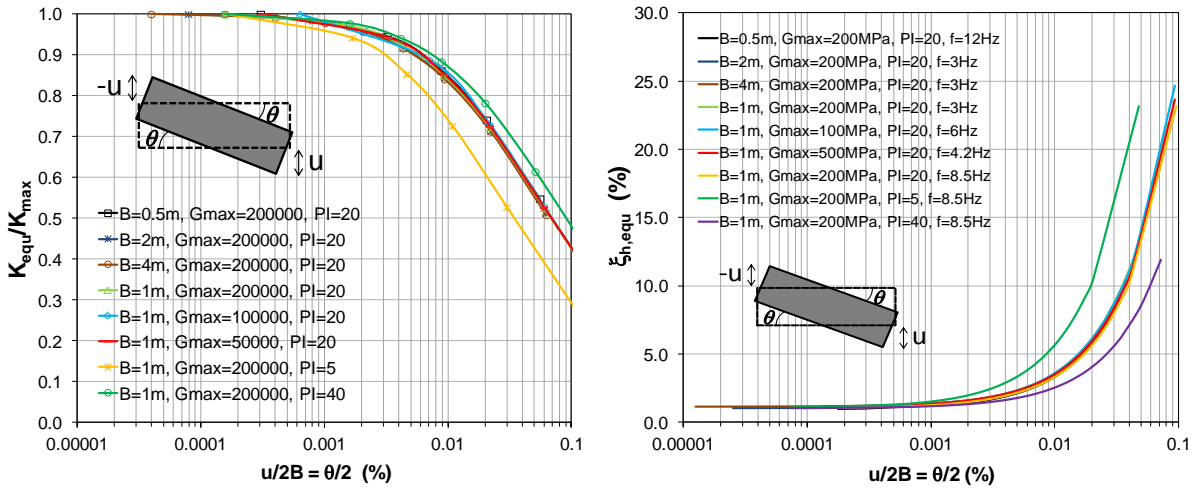


Figure 10. Equivalent spring stiffness K_{equ} and hysteretic damping ratio $\xi_{h, equ}$ as functions of the normalized footing edge displacement amplitude $u/2B$ for strip footing in rocking.

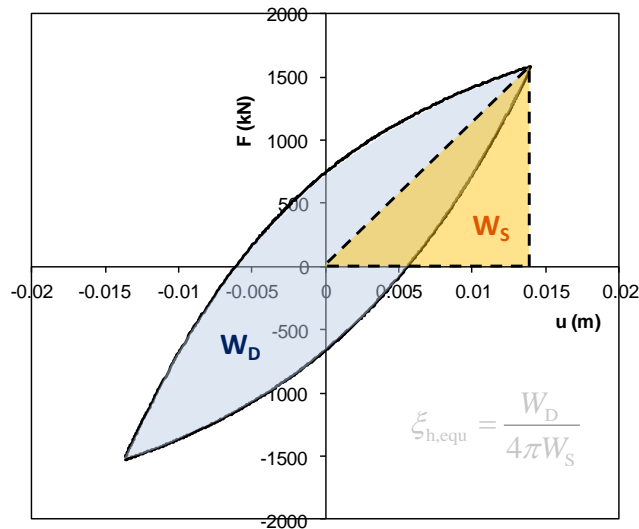


Figure 11. Typical hysteresis loop from quasi-static analysis of strip footing subjected to vertical cycling.

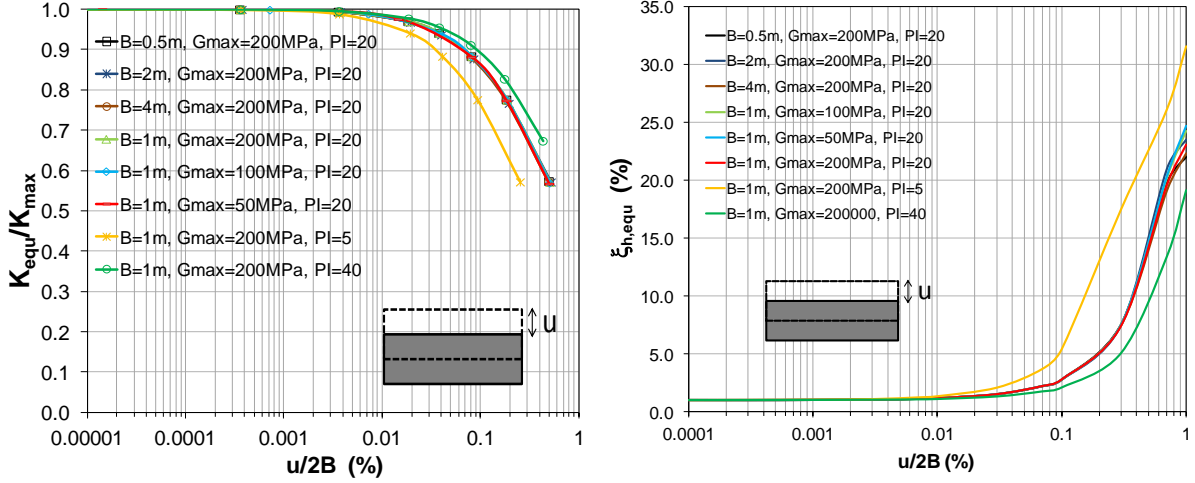


Figure 12. Equivalent spring stiffness K_{equ} and hysteretic damping ratio $\xi_{h,equ}$ as functions of the normalized footing displacement amplitude $u/2B$ for strip footing in vertical oscillation.

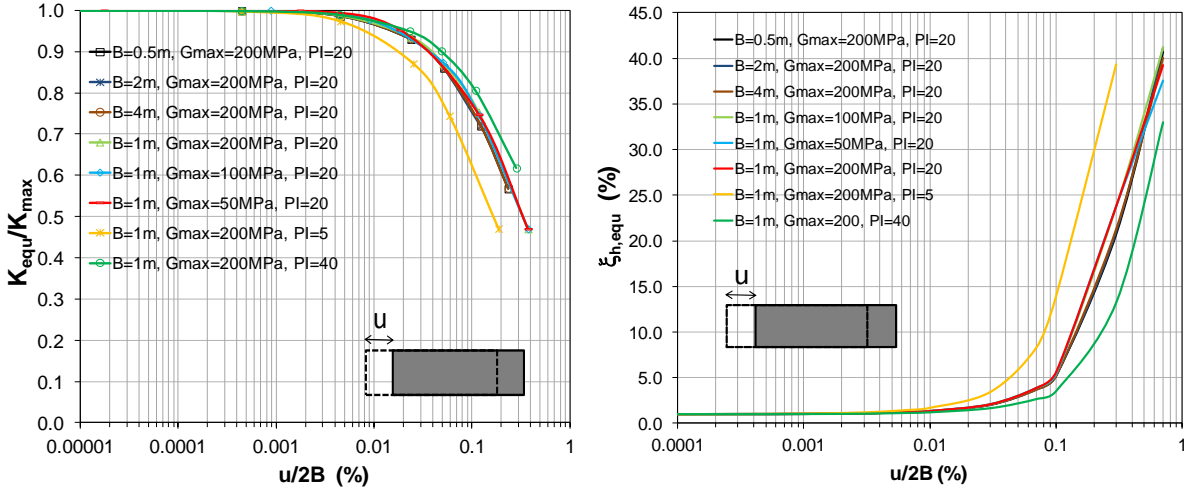


Figure 13. Equivalent spring stiffness K_{equ} and hysteretic damping ratio $\xi_{h,equ}$ as functions of the normalized footing displacement amplitude $u/2B$ for strip footing in horizontal oscillation.

The curves shown in Figs. 9, 10, 12 and 13 suggest that the equivalent stiffness reduction and the equivalent damping ratio depend solely on plasticity index PI . In particular, the reduction of K_{equ} and the increase of $\xi_{h,equ}$ with footing motion amplitude becomes less intense as PI increases, in much the same manner G and ξ_h at material point level depend on PI . In all examined modes, the curves are practically independent of the footing size and G_{max} . Moreover, the influence of oscillation frequency on $\xi_{h,equ}$ is insignificant.

For a given level of motion amplitude (say $u/2B=0.1\%$), $\xi_{h,equ}$ is much larger (and K_{equ}/K_{max} is much smaller) in the case of rocking than in the cases of vertical and horizontal oscillation. This can be attributed to the fact that the strains developing in the soil in the vicinity of the foundation in rocking are concentrated in a circular arc-shaped region immediately below the footing, where the soil is mostly sheared. In contrast, the vertical oscillation creates mainly longitudinal waves below the foundation and, to a lesser degree, shear waves that propagate diagonally and laterally, with the shearing diffusing gradually with depth. Horizontal oscillation generates mainly shear waves, but produces also longitudinal waves that propagate diagonally and laterally. As a consequence, the average shear strain in the foundation soil, for a given footing motion amplitude, is clearly larger in the case of rocking than in the case of vertical or horizontal oscillation. Thus, the effect of soil non-linearity (and hysteresis) is more pronounced in rocking than in any other mode. Yet, $\xi_{h,equ}$ is larger (and K_{equ}/K_{max} is smaller) in horizontal oscillation than in vertical oscillation. Hence, we can say that the

horizontal vibration case lies between rocking and vertical vibration in terms of importance of soil non-linearity.

CONCLUSIONS

A series of parametric analyses were performed using the finite element method (FEM) in order to determine equivalent values for the spring stiffness and hysteretic damping ratio that account for soil non-linearity in the standard spring-dashpot model. The finite element methodology was validated by first performing analyses in which the soil was linearly elastic with Rayleigh damping. Numerical results are in agreement with the predictions of the spring-dashpot model using coefficients based on semi-analytical solutions. It was observed that use of both mass and stiffness proportional Rayleigh damping leads to severe underestimation of the soil hysteretic damping. Hence, if possible, only stiffness proportional damping should be used in analyses involving wave generation and propagation in a continuum.

Finite element analyses performed assuming that the soil follows a hyperbolic stress-strain law with hysteresis show that the equivalent spring stiffness reduces and the equivalent (average) hysteretic damping ratio of the foundation-soil system increases with increasing motion amplitude, in practically the same manner as in the case of a sheared soil element. However, for the same order of displacement amplitude, the rocking mode exhibits significantly larger equivalent hysteretic damping ratio than the vertical or horizontal oscillation modes. Accordingly, the stiffness reduction is more intense in the case of rocking. Regardless of the type of oscillation, the equivalent spring stiffness reduction and hysteretic damping curves depend strongly on the plasticity index PI of the soil, but not on foundation size, maximum shear modulus or oscillation frequency.

Finally, the findings of the present study suggest that the effect of the foundation motion amplitude on the spring stiffness and dashpot coefficients is important and may result in a significant reduction of the spectral acceleration in soil-structure interaction computations, mostly due to the increased hysteretic damping ratio caused by the rocking mode. However, we must stress the fact that the constitutive model used herein to simulate non-linear soil behavior over-predicts significantly the hysteretic damping ratio at shear strain amplitudes larger than 0.1%, which may be operative in soil-structure interaction problems involving strong earthquake shaking. Hence, the findings reported in this paper need to be verified by analyses using a constitutive model that captures soil hysteresis accurately in the entire shear strain range.

REFERENCES

- Anastasopoulos I, Gazetas G, Loli M, Apostolou M, Gerolymos N (2010) "Soil failure can be used for seismic protection of structures", *Bulletin of Earthquake Engineering*, 8(2):309–326.
- Brinkgreve RBJ, Swolfs WM and Engin E (2011) PLAXIS 2D Reference manual, Delft, The Netherlands.
- Chatzigogos CT, Pecker A, Salencon J (2009) "Macroelement modeling of shallow foundations", *Soil Dynamics and Earthquake Engineering*, 29(5): 765–781.
- Cremer C, Pecker A, and Davenne L (2001). "Cyclic macro-element for soil–structure interaction: material and geometrical non-linearities" *International Journal for Numerical and Analytical Methods in Geomechanics*, 25(13): 1257-1284.
- Dobry R and Gazetas G (1986), "Dynamic response of arbitrarily shaped foundations", *Journal of geotechnical engineering*, 112(2): 109-135.
- Dobry R and Gazetas G "Dynamic response of arbitrarily shaped foundations." *Journal of geotechnical engineering* 112.2 (1986): 109-135.
- Dos Santos JA and Correia AG (2001) "Reference threshold shear strain of soil. Its application to obtain an unique strain-dependent shear modulus curve for soil", *Proceedings of the 15th International Conference on Soil Mechanics and Geotechnical Engineering*, Istanbul, Turkey, AA Balkema.
- Duncan JM and Chang C-Y (1970) "Nonlinear analysis of stress and strain in soils", *Journal of the Soil Mechanics and Foundations Division*, 96(5): 1629-1653.

- Gazetas GC and Roesset JM (1976) "Forced vibrations of strip footings on layered soils." *Methods of Structural Analysis*, ASCE: 115-131.
- Gazetas GC and Roesset JM (1979) "Vertical vibration of machine foundations" *Journal of the Geotechnical Engineering Division*, 105(12): 1435-1454.
- Gazetas G (1983) "Analysis of machine foundation vibrations: state of the art." *International Journal of Soil Dynamics and Earthquake Engineering* 2(1): 2-42.
- Gazetas G (1991) "Foundation vibrations", Chapter 15, *Foundation engineering handbook*, ed. Fang HY, Springer: 553-593.
- Hall JF. (2006) "Problems encountered from the use (or misuse) of Rayleigh damping." *Earthquake engineering & structural dynamics*, 35(5): 525-545.
- Houlsby GT, Cassidy MJ and Einav I (2005) "A generalised Winkler model for the behaviour of shallow foundations" *Géotechnique*, 55(6): 449-460.
- Karasudhi PL, Keer M and Lee SL (1968) "Vibratory motion of a body on an elastic half plane." *Journal of Applied Mechanics*, 35: 697-705.
- Kourkoulis R, Gelagoti F and Anastasopoulos I (2012) "Rocking isolation of frames on isolated footings: design insights and limitations" *Journal of Earthquake Engineering*, 16(3): 374-400.
- Kramer SL (1996) *Geotechnical earthquake engineering*, Prentice Hall.
- Luco JE and Westmann RA (1971) "Dynamic response of circular footings", *Journal of the Engineering Mechanics Division*, 97(5), 1381-1395.
- Lysmer J (1965) Vertical motion of rigid footings, Final Report. University of Michigan, Ann Arbor, Collection of Engineering.
- Mergos PE and Kawashima K (2005). "Rocking isolation of a typical bridge pier on spread foundation", *Journal of Earthquake Engineering*, 9(sup2): 395-414.
- Orologopoulos N (2013) Non-linear behavior and hysteretic damping of soils in the spring-dashpot model, MSc Thesis, University of Cyprus.
- Paolucci R (1997) "Simplified evaluation of earthquake-induced permanent displacements of shallow foundations" *Journal of Earthquake Engineering*, 1(3): 563-579.
- Veletsos AS and Wei YT (1971) "Lateral and rocking vibration of footings", *Journal of Soil Mechanics & Foundations Div*, 97(9): 1227-1248.
- Veletsos AS and Verbič B (1974) "Basic response functions for elastic foundations", *Journal of the Engineering Mechanics Division*, 100(2): 189-202.
- Vucetic M and Dobry R (1991) "Effect of soil plasticity on cyclic response", *Journal of Geotechnical Engineering*, 117(1): 89-107.
- Zafeirakos A and Gerolymos N (2013) "On the seismic response of under-designed caisson foundations", *Bulletin of Earthquake Engineering*, 11(5): 1337-1372.